a stint at the Petroleum Institute in Paris, he came to the University of Michigan, where his main interest is the rheology of viscoilastic fluids. After having been seduced into the area of membrane transport he has found it an ever-deepening and widening area of activity.

S. R. Suchdeo, has been an essential part of our effort. He came to Michigan via Bombay University and a M.S. from the University of Mississippi. As he has been involved in both the experimental and theoretical research he has provided some of the insights which ehlped our effort to obtain a broader perspective on the problem. He is now employed at Air Products and Chemicals, Allentown, Pennsylvania.

Scale-Up of Agitated Vessels Gas-Liquid Mass Transfer

Procedures are developed for predicting liquid film controlled mass transfer in gas sparged contactors with and without mechanical agitation. Mass transfer is shown to depend on mean bubble size. Bubble shape, motion, and interface fluctuations are all properties that are associated with bubble size, which, in turn, can be determined from the physical characteristics of the contacting system.

Experimental measurements were made on CO_2 stripping from aqueous solution with air in 0.00252, 0.0252, and 0.252 m^3 tanks. The vessels were geometrically similar, fully baffled, and equipped with four flat-blade impellers and spargers. These measurements are used to evaluate earlier correlations and to develop improved scale-up procedures.

DONALD N. MILLER

Engineering Department
E. I. du Pont de Nemours & Co., Inc.
Wilmington, Delaware 19898

SCOPE

One of the most frequent problems in chemical reactor design involves scale-up in which mass transfer has an important influence on overall rate. Reactions with interphase mass transfer are often carried out in agitated vessels. The selection of design and operating parameters necessary for reliable scale-up in units of this type is of particular importance.

Reference is made in this study to one important rate process—that of liquid film controlled mass transfer. This can be important in liquid-solid, liquid-liquid, and gas-liquid contacting. Among these systems, analysis of performance is simplest for liquid-solid mass transfer because the size of the particulate phase can be independently controlled. Analysis with gas-liquid contacting is the most complicated. This is true because certain properties of the dispersed phase that affect mass transfer—bubble size, shape, motion and the frequency and extent of interface fluctuations—are determined by the contacting system itself.

The first consideration in agitated vessel scale-up is maintenance of geometric similarity. This requires that all corresponding linear dimensions in two vessels of different size be in the same ratio. Beyond this, for gas-liquid systems, there is the question of selecting an appropriate sparger design. Further, if mechanical agitation is imposed, a choice must be made of the proper impeller speed.

This study was undertaken to relate liquid film controlled mass transfer to the established physical characteristics of sparged and mechanically agitated systems. The ultimate objective through this analysis is to identify the appropriate scale-up requirements.

CONCLUSIONS AND SIGNIFICANCE

It is important in the scale-up and design of gas-liquid reaction equipment to be able to predict mass transfer rates reliably. Procedures have been developed for calculating liquid film controlled mass transfer in gas sparged systems both with and without mechanical agitation. These procedures are based on experimental measurements of the stripping of CO_2 from aqueous solution with air.

Liquid film controlled mass transfer in gas-liquid contacting is shown to depend on mean bubble size. Bubble shape, motion, and any tendency for the interface to ripple, fluctuate, or otherwise deform might also be expected to influence mass transfer. These effects are all related to bubble size, however, which in turn is determined by the physical characteristics of the contacting system.

After leaving the sparger in a gas-liquid contactor, bubbles either break up or coalesce as they move upward through the bulk liquid, shifting toward an equilibrium size limit. Mean bubble size can be approximated by taking the geometric mean between the bubble size produced at the sparger and the equilibrium bubble size.

Most commercial scale spargers operate in the turbulent chain bubbling flow regime. Within this flow regime, bubble size depends on the volumetric gas flow rate through each sparger opening and is independent of hole dimensions. Equilibrium bubble size is primarily dependent on the energy content of the liquid phase.

When mechanical agitation is imposed in a sparged system, it augments the energy content of the liquid phase and bubble size is reduced. With this situation, the separate power input contributions of gas sparging and mechanical agitation must be combined in an effective, overall value for use in prediction of bubble size.

Mechanically agitated vessels under 0.25 m^3 in size require correction for surface aeration. A correction term is derived based on impeller tip speed, superficial sparged gas velocity, and clear liquid depth above the impeller. This can be applied to the sparged gas rate as a multiplying factor to obtain total gas input inclusive of both sparging and surface entrainment.

Geometric similarity and equal effective power input, combining sparged gas and mechanical energy sources, are the basic requirements for duplicating liquid film controlled mass transfer in scale-up. This would be true

without further qualification if mean bubble equalled equilibrium bubble size in the systems being scaled. In any practical situation, however, bubble sizes are intermediate, between those at the sparger and at equilibrium. As a result, for the usual turbulent chain bubbling gas distribution, there is a third requirement for precise scale-up: volumetric gas flow rates through the individual sparger openings must be kept constant.

THEORETICAL BACKGROUND

Mass Transfer

The Boussinesq equation (Boussinesq, 1905) is used to characterize mass transfer in gas-liquid contacting:

$$N_{Sh} = \sqrt{\frac{4}{\pi}} N_{Pe}^{1/2} \qquad (1)$$

This equation was developed for a fluid in potential flow with a short interface contact time. It will be assumed that both N_{Sh} and N_{Pe} include mean bubble diameter D_{BM} as the length parameter. D_{BM} is the diameter of equal size spheres having the same total surface area as the actual bubbles in a system, whatever may be their true shape and size distribution. This is sometimes referred to as the surface volume mean or Sauter diameter.

If contact time t_e is assumed equal to the time it takes a bubble to rise one bubble diameter and D_{BM}/t_e is substituted for u_t in Equation (1), it reduces to the penetration theory expression

$$k_L = \sqrt{\frac{4D}{\pi t_e}} \qquad (2)$$

The physical concept behind penetration theory is that there is a continual attachment and detachment of small liquid eddies at the gas-liquid interface. In the interval of attachment, there is an interchange of solute by molecular diffusion.

These are idealized relationships that apply in air-water contacting, for example, if mean bubble diameter is about 0.0075 m. With larger bubbles, more surface disturbances can occur, mass transfer is enhanced and Equation (1) is conservative.

Conversely, Equation (1) predicts too high a mass transfer characteristic for smaller bubbles. Very small bubbles tend to approach a rigid spherical configuration at which condition they behave as solid particles. Boundary layer theory applies for mass transfer at this extreme. Procedures for predicting liquid film controlled mass transfer with a solid particulate phase are available elsewhere (Miller, 1967, 1971).

The experimental work to be described defines a correction term k_L^* with which Equation (1) can be made generally applicable for bubble sizes above 0.004 m. The k_L^* factor is a function of mean bubble size D_{BM}, which is determined by the properties of the contacting system.

Two-Phase Flow Regimes

At low gas flow rates, as shown by Van Krevelen and Hoftijzer (1950), bubbles form as single entities at a sparger orifice, and bubble size is a function of the orifice size,

$$D_B = 1.817 \left(\frac{\sigma d_o}{g(\rho_l - \rho_g)} \right)^{1/3} \qquad (3)$$

As gas flow rate is increased, a point is reached at which bubble formation is hindered by the presence of preceding bubbles. Bubble size then increases as much as is necessary to carry the amount of gas sparged and becomes a function of gas flow rate rather than orifice size. This is called *chain bubbling*.

Two regimes of flow in chain bubbling are distinguished: laminar, at bubble Reynolds numbers N_{Reb} less than 9; and turbulent at N_{Reb} greater than 9.

In the laminar region of chain bubbling, bubble size is a function of the ¼ power of gas flow rate,

$$D_B = 3.22 \left(\frac{\mu_l}{\pi g(\rho_l - \rho_g)} \right)^{0.25} Q_g^{0.25} \qquad (4)$$

In turbulent chain bubbling, bubble size is a function of the 0.4 power of gas flow rate,

$$D_B = 2.35 \left(\frac{\rho_l}{\pi^2 g(\rho_l - \rho_g)} \right)^{0.2} Q_g^{0.4} \qquad (5)$$

These relationships are shown on the Figure 1 plot of expansion number Ex vs. bubble Reynolds number. The expansion number multiplied by the factor 4/3 equals the drag coefficient C_D. It is analogous to the Fanning friction factor for flow in pipes but is more complicated, involving form as well as skin drag.

If gas flow rate is increased still further, a transition occurs to a spiraling jet of fine bubbles. This is called spouting. Leibson et al. (1956) have studied air-water spouting. Their plot of mean bubble diameter vs. orifice Reynolds number in Figure 2 shows this transition to occur in the range $2000 < N_{Re_0} < 10{,}000$.

Bubble Motion

The characteristics of rising gas bubbles above the point of sparging have been studied extensively (Datta et al., 1950; Haberman and Morton, 1953). Figure 3 shows a plot of terminal velocity of rise for air bubbles in pure water vs. mean bubble diameter. Also indicated are the regions of different bubble motions designated by

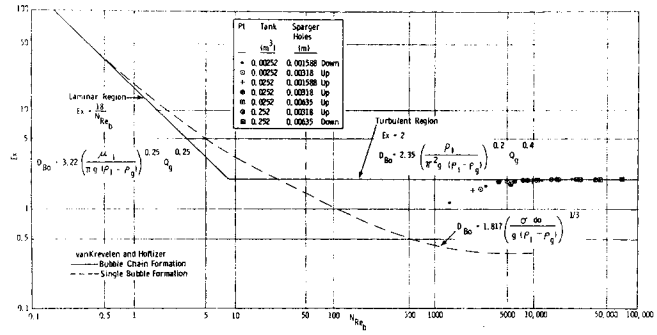

Fig. 1. Expansion number vs. bubble Reynolds number.

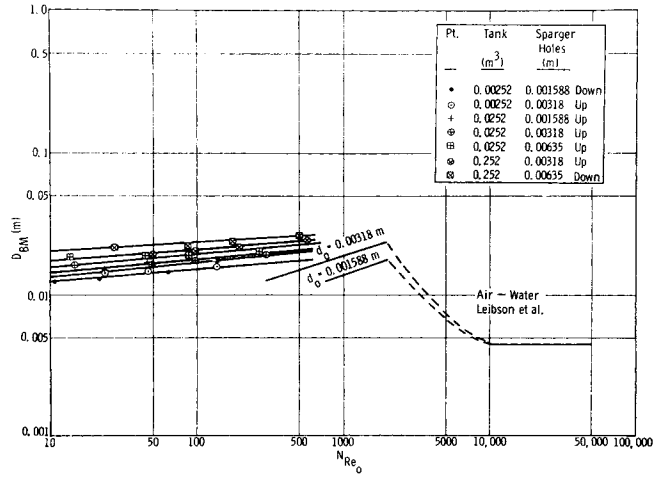

Fig. 2. Mean bubble diameter vs. orifice Reynolds number.

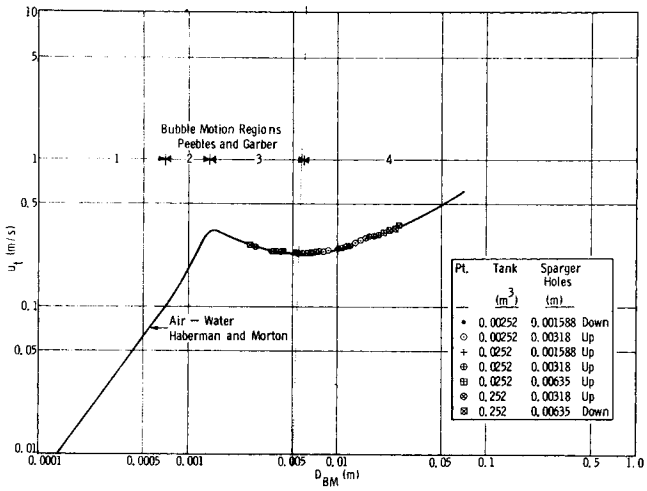

Fig. 3. Terminal velocity of rise vs. mean bubble diameter for air-water.

Peebles and Garber (1953). These are:

Region 1 ($D_{BM} < 0.0007$ m): Bubbles behave as solid spheres and their velocity of rise is consistent with Stoke's law.

Region 2 (0.0007 m $< D_{BM} <$ 0.0014 m): Bubbles remain spherical but some internal circulation occurs, reducing shear stress at the interface, and velocity of rise is higher than predicted by Stoke's law.

Region 3 (0.0014 m $< D_{BM} <$ 0.006 m): Bubbles are no longer spherical and follow a zigzag or helical upward path. Viscous drag is augmented by vortex formation in the wake, and velocity of rise remains fairly constant over the bubble size range.

Region 4 ($D_{BM} > 0.006$ m): Bubbles assume a spherical cap shape, and terminal bubble velocity tends to increase gradually with increase in bubble size.

The usual well-designed commercial sparger operates within the turbulent chain bubbling flow regime and bubble motion falls within Regions 3 and 4. The experimental points in Figures 1, 2, and 3 are those of this study.

Prediction of Mean Bubble Size, Gas Holdup, and Interfacial Area

Gas Sparging With no Mechanical Agitation. As bubbles leave the immediate vicinity of a sparger, there are adjustments in diameter, through coalescence or break-up, and they approach an equilibrium size distribution. A stable size is achieved when turbulent fluctuations and surface tension forces are in balance (Hinze, 1955; Calderbank, 1959). Viscous forces do not influence this balance significantly unless the dynamic pressure fluctuations are unusually severe.

Lehrer (1971) recommends that the geometric mean between bubble diameters at the sparger orifice D_{BO} and stable bubble diameter D_{BE} be used to characterize gas sparged systems with no mechanical agitation

$$D_{BM} = (D_{BO}\, D_{BE})^{1/2} \tag{6}$$

Assuming $\rho_l >> \rho_g$, for chain bubbling,

$$D_{BO} = 2.05 \left\{ \frac{Q_g}{\pi N_o'} \right\}^{0.4} \left\{ \frac{3\, C_D}{4\, g} \right\}^{0.2} \tag{7}$$

where $C_D = 8/3$ for turbulent chain bubbling and $C_D = 24/N_{Reb}$ for laminar chain bubbling. N_o' incorporates a correction for coalescence due to bubble overlap at the sparger. If $D_{BO}/0.75$ is less than X, the spacing between sparger holes, N_o' equals N_o the actual number of holes. If $D_{BO}/0.75 \geq X$, N_o' for a perforated pipe sparger is

$$N_o' = \frac{\{(N_o - 1)X + D_{BO}/0.75\}}{D_{BO}/0.75} \tag{8}$$

For a perforated plate design, Equation (8) applies in squared form.

The stable bubble diameter is

$$D_{BE} = 3.48\, C_D^{-0.6} \left(\frac{\sigma^{0.6}}{(P_g/V)^{0.4}\, \rho_l^{0.2}} \right) \tag{9}$$

Attainment of D_{BE} is presumed to require high turbulence in the immediate vicinity of a bubble, for which $C_D = 8/3$.

Gas holdup ϕ can be estimated from

$$\phi = \frac{u_g}{u_t + u_g} \tag{10}$$

Mendelson's wave equation predicts the terminal velocity of bubble rise u_t (Mendelson, 1967),

$$u_t = \left\{ \frac{2\sigma}{\rho_l\, D_{BM}} + \frac{g\, D_{BM}}{2} \right\}^{0.5} \tag{11}$$

Interfacial area

$$a = 6\, \phi / D_{BM} \tag{12}$$

Lehrer's prediction methods apply where liquid depth is equal to or greater than vessel diameter, the liquid is not highly viscous, and there are no wall effects.

Gas Sparging With Mechanical Agitation

Calderbank's equations modified for high gas sparging rates with mechanical agitation follow (Calderbank, 1958):

$$D_{BM} = 4.15 \left(\frac{\sigma^{0.6}}{(P_e/V)^{0.4}\, \rho_l^{0.2}} \right) \phi^{0.5} + 0.0009 \tag{13}$$

$$\phi = \left(\frac{\phi\, u_g}{u_t + u_g} \right)^{0.5} + 0.000216 \left(\frac{(P_e/V)^{0.4}\, \rho_l^{0.2}}{\sigma^{0.6}} \right) \left(\frac{u_g}{u_t + u_g} \right)^{0.5} \tag{14}$$

$$a = 1.44 \left(\frac{(P_e/V)^{0.4}\, \rho_l^{0.2}}{\sigma^{0.6}} \right) \left(\frac{u_g}{u_t + u_g} \right)^{0.5} \tag{15}$$

The modifications include use of Equation (10) for fractional gas holdup and an effective power input P_e/V. This latter term combines both gas sparging and mechanical agitation energy contributions. The original equations were based on mechanical P_m/V alone and apply only at low gas rates ($u_g < 0.02$ m/s). Supporting data were obtained at low air sparging rates in ten different liquids. Liquid surface tensions ranged from 0.0217 to 0.0735 N/m; densities from 790 to 1600 kg/m³; and viscosities from 0.0005 to 0.028 N · s/m². No liquid viscosity effect was shown within the range tested.

There is a tendency in agitated systems for gas to be entrained at the top liquid surface. The amount of gas picked up at the surface can be significant for vessels under 0.25 m³ in size. The entrained gas circulates along with sparged gas in the aerated mass, and it is the combined gas velocity that is operative as a correlating parameter in Calderbank's equations.

The influence of surface entrainment on interfacial area was studied by Calderbank in 0.02, 0.04, and 0.1 m³ tanks (Calderbank, 1959). Experimental data were correlated with the collection of terms $N_{Rei}^{0.7}\ \{nd/u_g\}^{0.3}$. Although applicable within the range of vessel parameters studied, this correlation is not useful for scale-up. The

impeller Reynolds number N_{Rei} increases with impeller diameter d, and, as a result, the predicted interfacial areas also increase with increase in vessel size. The development of an aeration correction correlation for scale-up will be discussed in the experimental section which follows.

Power Input

Power input to the liquid phase in a sparged system can be calculated from

$$P_g/V = \frac{Q_g \rho_g}{V}\left\{\frac{\eta u_o^2}{2} + \frac{RT}{M}\ln\left(\frac{\pi_o}{\pi}\right)\right\} \qquad (16)$$

This expression is derived by Lehrer (1968). The first term in brackets represents jet energy developed at the sparger holes and transmitted to the bulk liquid. The second term is energy required to move the gas through the static liquid head above the sparger. For well-designed spargers, the first term is often small and can be neglected.

Mechanical power input in a sparged, agitated system can be calculated from

$$P_m/V = \frac{0.706}{V}\left\{\frac{P^2{}_{mo}\, nd^3}{Q_g{}^{0.56}}\right\}^{0.45} \qquad (17)$$

This expression is recommended by Michel and Miller (1962). Unaerated mechanical power input can be obtained from

$$P_{mo}/V = \frac{fn^3d^5\rho_l}{V} \qquad (18)$$

The power factor f is available through the work of Rushton et al. (1950) and O'Connel and Mack (1950).

The power input term in Calderbank's equations for D_{BM}, ϕ, and a combines both sparged gas and mechanical energy contributions. Although each can be predicted as a separate effect, their combination is not simply additive. Effective power input can be estimated from

$$P_e/V = P_m/V + C_1 P_g/V \qquad (19)$$

The C_1 correction term can be obtained by comparing D_{BM} for gas sparging only as calculated from Equations (6) and (13). In the latter case, P_m/V is zero and the effective power input P_e/V equals $C_1 P_g/V$. By making trial and error adjustments of C_1 until D_{BM} from Equation (13) matches D_{BM} from Equation (6), the appropriate C_1 value can be determined. The C_1 values obtained in this study are plotted in Figure 4 as functions of vessel size and sparger characteristics.

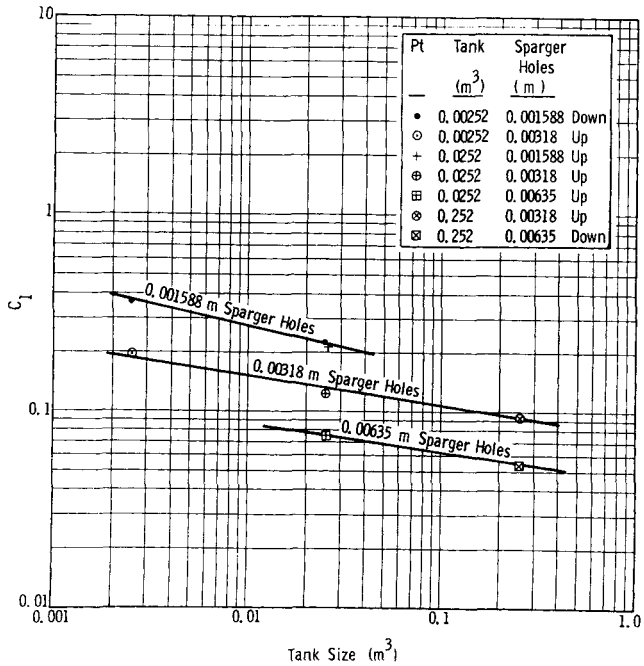

Fig. 4. Power input correction factor.

EXPERIMENT

Vessels

Three tanks were used in this study. Design details are shown in Figure 5. Dimensions are given in Table 1.

Each tank was fitted with a ring sparger located under the agitator impeller. To fully contain the froth height and avoid splash-over under aerated conditions, all experimental runs were made with water levels at the center overflow nozzles. Nominal clear liquid holdups for the three vessels are 0.00252, 0.0252, and 0.252 m³. All linear dimensions are in the ratios 1:2:4.5.

The tanks are fully baffled. Agitators are four-blade, flat paddles. The agitator speed ranges are 2.83 to 7.0 s^{-1} in the 0.00252 m³ tank; 1.717 to 7.0 s^{-1} in the 0.0252 m³ tank; and 0.417 to 2.80 s^{-1} in the 0.252 m³ tank. Bottom dished heads are consistent with standard ASME specifications.

Spargers

Sparger hole dimensions, spacing, and orientation are given in Table 2. All sparger designs were planned to provide effective lateral distribution over the full range of gas rates to be studied.

The numbers of sparger holes for the small tank designs were chosen to keep maldistribution within 10%. The numbers of sparger holes for the larger tank designs were chosen

Table 1. Vessel Dimensions

	Nominal vessel size, m³		
	0.00252	0.0252	0.252
	Dimensions, m		
A	0.1524	0.305	0.686
B	0.1460	0.292	0.657
C	0.305	0.610	1.372
D	0.1016	0.203	0.457
E	0.01905	0.0381	0.0857
F	0.000794	0.001588	0.00357
G	0.00952	0.01905	0.0429
H	0.00952	0.01905	0.0429
I	0.01270	0.0254	0.0572
J	0.001588	0.00318	0.00714
K	0.01270	0.0254	0.0572
L	0.0889	0.1778	0.406
M	0.01270	0.0254	0.0508
N	0.000889	0.001245	0.00212

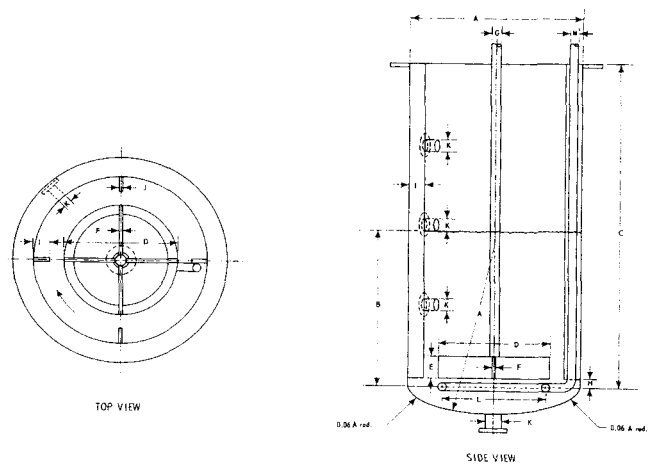

Fig. 5. Vessel design.

Table 2. Sparger Hole Dimensions

	Nominal vessel size, m^3						
	0.00252		0.0252		0.252		
	Dimensions, m						
Hole size	0.001588	0.00318	0.001588	0.00318	0.00635	0.00318	0.00635
No. holes	40	10	80	20	10	50	25
Hole spacing	0.00698	0.0279	0.00698	0.0279	0.0559	0.0260	0.0518
Orientation	Down	Up	Up	Up	Up	Up	Down

to keep close to the same hole spacing for corresponding hole sizes.

This is common scale-up procedure. Gas distribution improves with increasing vessel size. The number of sparger holes per unit vessel cross section decreases, however. Gas flow rate per sparger hole therefore increases with increasing vessel size, and, as will be shown, mass transfer is adversely affected.

Procedure

The stripping of CO_2 from aqueous solution with air, a liquid film controlled rate process, was used to characterize mass transfer performance. Feed solution for each experimental run was first saturated with CO_2 in a hold tank. It was then pumped up into the bottom center nozzle of each test vessel and allowed to overflow through the side, center nozzle. Air was put through the sparger and CO_2 depletion measured by sampling and analyzing the feed and effluent streams.

Time intervals sufficient for several displacements of the liquid holdup were allowed before sampling. Three samples of both inlet and effluent solution were taken and the results averaged for each run. Analyses were made with a portable Beckman *p*H meter, titrating with standard NaOH to the equivalent of a phenolphthalein end point.

Check samples taken at the lower nozzles and, by dip tube, just above the impellers showed no significant vertical concentration gradients on the various runs. Blank samples of the fresh water feed were analyzed for acidity prior to saturating each new batch of feed solution. The equivalent CO_2 contents of these blanks were in all cases very small relative to the subsequent CO_2 test measurements.

Mass transfer rate constants were calculated from the following relationship:

$$k_L a = \frac{Q_l(c_i - c_o)}{V_a c_o} \tag{20}$$

CO_2 concentrations in the effluent gas phase were negligibly small in all cases so that the liquid interface CO_2 concentrations were effectively zero.

In addition to the mass transfer measurements, the fraction gas holdup was determined on each run. Air rate, water rate, and agitator speed were set at the desired conditions and liquid holdup allowed to equilibrate. The straight side froth height was then measured. Air, water, and agitator were next turned off and the gas allowed to disengage. The straight side clear liquid height was then measured. From the straight side height measurements and vessel dimensions, including bottom head volume, both aerated and clear liquid volumes were calculated. Fraction aeration was then determined from

$$\phi = \frac{V_a - V}{V_a} \tag{21}$$

Seven run series were made, each with a different tank and sparger combination. Within each run series, one run was made with the agitator off and several at different speeds with the agitator on. The water rate for each run was chosen to permit accurate mass transfer determinations; that is, so that effluent CO_2 concentrations were high enough for analytical accuracy, yet low enough for a measurable $c_i - c_o$ differential. Four air rates were used on each run. These were chosen to give superficial gas velocities of 0.00762, 0.0254, 0.0508, and 0.1524 m/s.

ANALYSIS OF RESULTS

Experimental values of k_L were obtained for all the runs by dividing the measured k_La's by the appropriate interfacial areas as calculated from Equations (12) or (15). Mass transfer coefficients via Equation (2) were also calculated for all the experimental runs. By ratioing the experimental to calculated values, reduced mass transfer coefficients were obtained:

$$k_L^* = \frac{k_{L\ \mathrm{exp}}}{k_{L\ \mathrm{calc}}} \tag{22}$$

In making these calculations, surface tensions for air-water and diffusivities for CO_2 in water were taken from standard sources (*International Critical Tables*, 1928, a and b).

The reduced coefficients were found to range between 0.1 and 10. Corresponding bubble diameters ranged from 0.00254 to 0.0254 m. The reduced coefficient k_L^* can be applied as a correction factor to Equation (1).

Correlation of k_L^* with D_{BM} was found to be particularly good for the 0.252 m^3 mechanically agitated tank results, along with those obtained in all three tanks with gas sparging alone. Deviations of smaller tank, mechanically agitated k_L^*'s are explainable as surface aeration effects.

For these smaller tank results, Q_g in Equation (17) and u_g in Equations (14) and (15) were adjusted with a common multiplying factor C_2 to reflect total gas input inclusive of both sparging and surface entrainment. C_2's for each experimental run were adjusted by trial and error. The corresponding k_L^* and D_{BM} values were recalculated via Equations (22) and (13) until the best fit of all the data was obtained.

Aeration correction factors were correlated with impeller tip speed and superficial sparged gas velocity through the Strouhal number

$$N_{SI} = \frac{\pi d n}{u_g} \tag{23}$$

and with clear liquid depth above the impeller Z:

$$Y = N_{SI}^{0.13}/Z^{0.87} \tag{24}$$

$$C_2 = 0.348\,Y \quad \text{for} \quad Y > 2.81 \tag{25}$$

$$C_2 = 1.0 \quad \text{for} \quad Y \leq 2.81 \tag{26}$$

Final results are shown in Figure 6. The best fit relationship is

$$k_L^* = 683\,D_{BM}^{1.376} \tag{27}$$

The mean deviation of experimental points is ± 16.1%, and the square of the multiple correlation coefficient R_A^2 is 0.928. This latter number is the fractional improvement afforded by the use of the correlation over use of a mean value for all experimental points. A coefficient 1.0 represents perfect correlation; zero, no improvement over the

mean.

The dependence of k_L^* on D_{BM} follows the expected trend. The larger the bubble size, the greater the frequency and extent of surface deformations. Liquid film controlled mass transfer is enhanced by these interface fluctuations.

The smaller the bubble size, the closer the approach to a rigid, spherical configuration. At this end of the bubble size spectrum, boundary layer theory and the Frössling equation apply (Frössling, 1938).

$$N_{Sh} = 2 + N_{Reb}^{1/2} N_{Sc}^{1/3} \qquad (28)$$

Neglecting the first term 2 and calculating k_{LF} from Equation (28), it can be shown that

$$k_L^* = \frac{k_{LF}}{k_{L\ \text{calc}}} = 0.97\, N_{Sc}^{-1/6} \qquad (29)$$

For mass transfer of CO_2 in air-water systems at ambient temperatures, k_L^* for rigid spherical bubbles is 0.33 for which D_{BM} is about 0.00381 m.

DISCUSSION

Figure 7 shows a plot of k_La for CO_2 in water at 20°C vs. impeller speed with superficial sparged gas velocity as parameter. The latter variable, designated as $C_2\ u_g$, has been corrected to include the surface aeration component. The curves have been calculated; the points are experimental.

The corresponding relationships for ϕ are shown in Figure 8. Both k_La and ϕ increase with increasing gas rate and agitator speed. Gas sparging is the stronger effect and tends to be increasingly dominant as gas rate increases. At superficial gas velocities 0.15 m/s and higher, very little additional mass transfer improvement can be gained with increased mechanical energy input. No effects of sparger hole orientation up or down could be detected within the range of experimental accuracy.

The horizontal portions of the curves to the left represent regions where agitator speeds are low and the mechanical energy contribution to mass transfer is not significant. In these regions, three curves are shown for each gas rate. These correspond to the three different size tanks used in this study.

Both k_La and ϕ decrease with increasing tank size. This illustrates the usual full-scale plant characteristic. As vessel size is increased, fewer sparger holes are needed per unit cross section for good gas distribution. With fewer sparger holes, gas rate per sparger hole is greater, and the mean bubble diameter is larger. This causes k_L to increase, but ϕ and a both diminish. The decrease in a is the stronger effect relative to k_L, and k_La therefore decreases as gas flow rate through each sparger opening is increased.

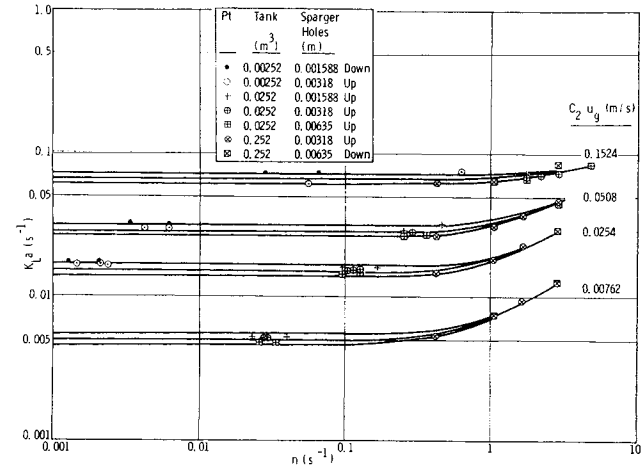

Fig. 7. $K_L\ a$ vs. agitator impeller speed n and superficial gas velocity C_2u_g for CO_2 from air in water at 20°C.

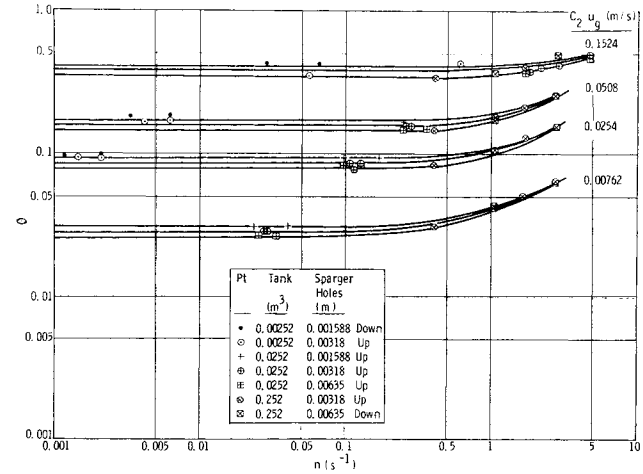

Fig. 8. ϕ vs. agitator impeller speed n and superficial gas velocity C_2u_g for air-water at 20°C.

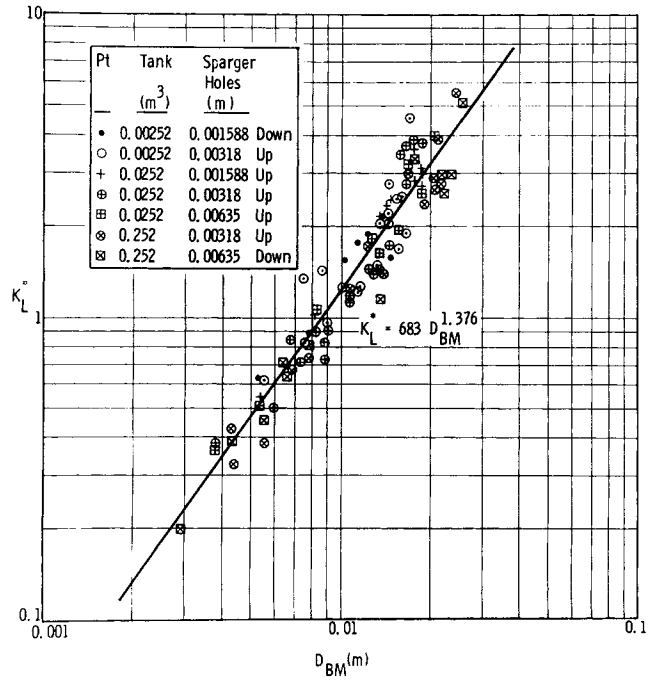

Fig. 6. K_L^* vs. D_{BM}.

COMPARISONS WITH OTHER PUBLISHED CORRELATIONS

Mean Bubble Size

Vermeulen and co-workers (1955) developed a correlation for bubble and drop diameters in agitated tanks based on light transmission measurements. Prior knowledge of the volume fraction of dispersed phase is required:

$$D_{VM} = \frac{0.00429\ \sigma\ \mu_l^{0.25}\ \Phi}{n^{1.5}\ d\ \rho_l^{0.5} \mu_g^{0.75}} \qquad (30)$$

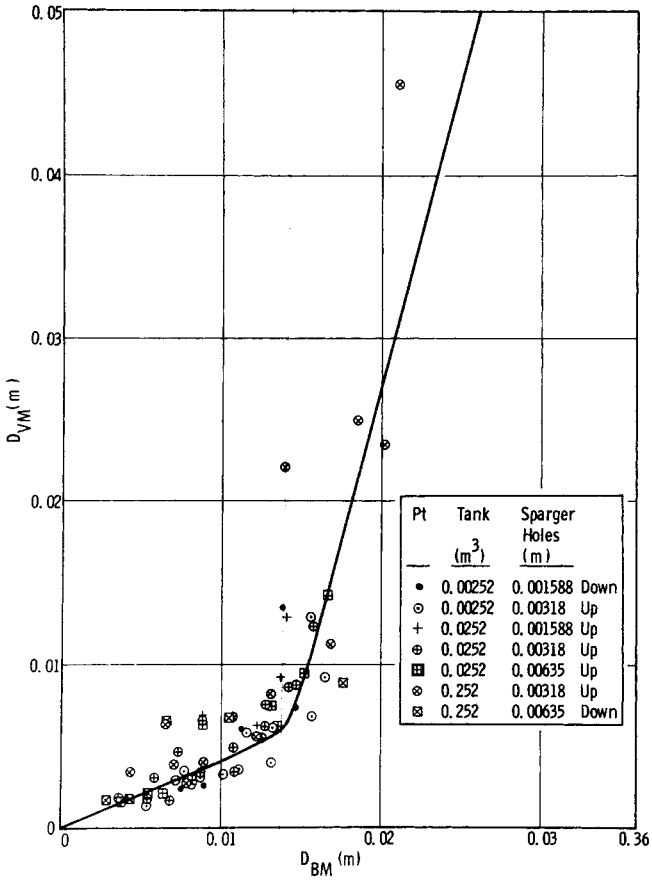

Fig. 9. Vermeulen bubble size—D_{VM} vs. D_{BM}.

where

$$\Phi = \exp\left[1.072 + 0.626 \ln \phi + 0.0733 (\ln \phi)^2\right]$$

Values of D_{VM} are plotted vs. the corresponding D_{BM} values of this study on Figure 9. The former tend to be low for most conditions, apparently because the Vermeulen measurements were made close to the impellers. Bubbles in this region have not started to equilibrate and their size is not representative of overall tank characteristics.

D_{VM} becomes disproportionately large at impeller speeds under 1.5 s^{-1}; and approaches infinity as n goes to zero.

Gas Holdup

Clark and Vermeulen (1963) correlated gas holdup data in sparged agitated tanks by segregating an incremental, mechanically-induced term $\Delta\phi$:

$$\phi = \phi_o + \Delta\phi \qquad (31)$$

The variable ϕ_o represents fractional gas holdup produced by sparging alone. The ϕ_o data of this study are shown in Figure 10. The corresponding Clark-Vermeulen dashed curve falls below these data at superficial gas velocities above 0.008 m/s.

Clark and Vermeulen correlated $\Delta\phi$ in the following collection of variables as a function of superficial gas velocity,

$$\phi' = \Delta\phi (W/H)^{-2/3} N_{We_i}^{-3/4} (P_m/P_{mo}^*)^{-1/2} \qquad (32)$$

The $\Delta\phi$ data of this study were found to correlate best with

$$\phi' = \Delta\phi\, W^{-1.235} H^{1.933} N_{We_i}^{-0.537} \qquad (33)$$

as a function of $C_2\, u_g$. The power input ratio is not a significant variable. As indicated by the scatter of points in Figure 11, resolution via this correlation procedure is poor. The mean deviation of experimental points is ± 39.6%; the square of the multiple correlation coefficient is 0.721.

Interfacial Area

Westerterp et al. (1963) report the following correlation for interfacial areas in sparged tanks:

$$aH = 800\, \mu_l\, (n - n_o)\, d\, (d/T)^{1/3} \left(\frac{\rho_l T}{\sigma}\right)^{1/2} \qquad (34)$$

Experimental k_La values were obtained by measuring rates of absorption of oxygen in sodium sulfite solutions with cupric sulfate as catalyst. If it is assumed that the sulfite reaction is fast, occurring in the liquid film, the effective mass transfer coefficient can be shown to be a function of the oxygen diffusivity and reaction rate constant and to be independent of any of the hydrodynamic

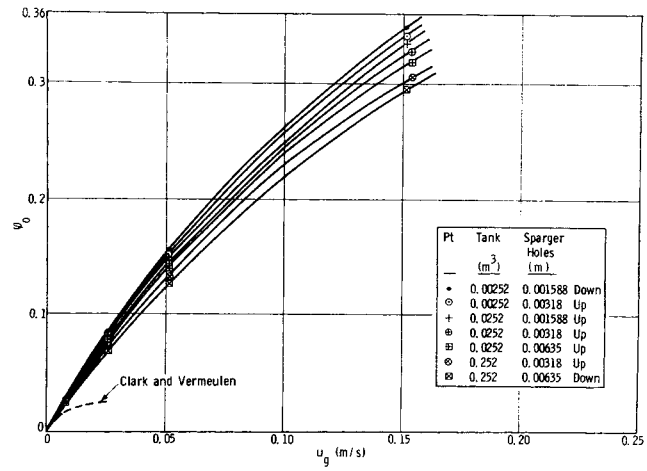

Fig. 10 ϕ_o for gas sparging vs. superficial gas velocity u_g for air-water at 20°C.

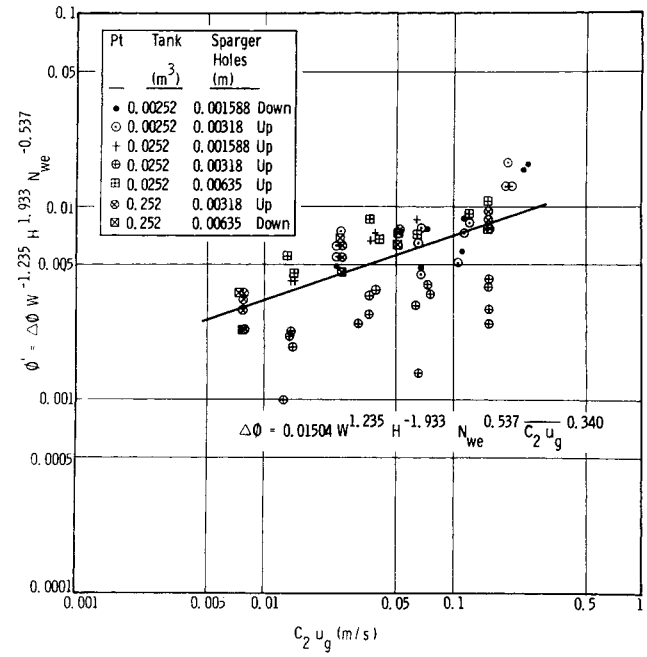

Fig. 11. ϕ' vs. superficial gas velocity $C_2 u_g$.

properties of the system (Astarita, 1967):

$$k_L = \left\{ \frac{2\,D\,k\,(c^* - c)^{n-1}}{n+1} \right\}^{1/2} \qquad (35)$$

Westerterp assumed first-order reaction, made an independent determination of D and k, and applied k_L from Equation (35) to segregate interfacial areas from his experimental k_La values. As it turns out, the copper catalyzed sulfite oxidation is too slow to satisfy the liquid film reaction assumption; and Westerterp's interfacial areas, determined by this "chemical method", are too low by an order of magnitude (Linek, 1966; Wesselingh and van't Hoog, 1970). Westerterp's Equation (34) correlation, however, is of particular interest.

The data of this study showed ΔaH rather than aH in Equation (34) to be the more appropriate correlating term. The variable Δa is the mechanically-induced increment in total interfacial area. Interfacial areas a_o for gas sparging obtained in this study are shown in Figure 12.

The ΔaH plot is given in Figure 13. The term d/T is omitted as a correlating parameter because it was not varied on any of the experimental runs in this study. As indicated, ΔaH is zero at the intercept 0.01458 N · s/m² on the abscissa. This defines n_o, the agitator speed, below which mechanical agitation has no significant effect on interfacial area, as

$$n_o = \frac{0.01458}{\mu_l\, d \left(\frac{\rho_l T}{\sigma}\right)^{1/2}} \qquad (36)$$

The final correlation is

$$\Delta aH = 1150\,\mu_l\,(n - n_o)\,d\left(\frac{\rho_l T}{\sigma}\right)^{1/2} \qquad (37)$$

for which the mean deviation of experimental points is ± 39.6, and the square of the multiple correlation coefficient is 0.898.

RECOMMENDATIONS

Equation (1) corrected for bubble size with Equation (27) is recommended for predicting mass transfer performance in sparged contactors.

Bubble size, gas holdup, and interfacial area for chain bubbling can be predicted from Equations (6) through (12). If mechanical agitation is superimposed, Equations (13) through (15) apply. For agitated vessels under 0.25 m³ in size, surface aeration should be taken into account

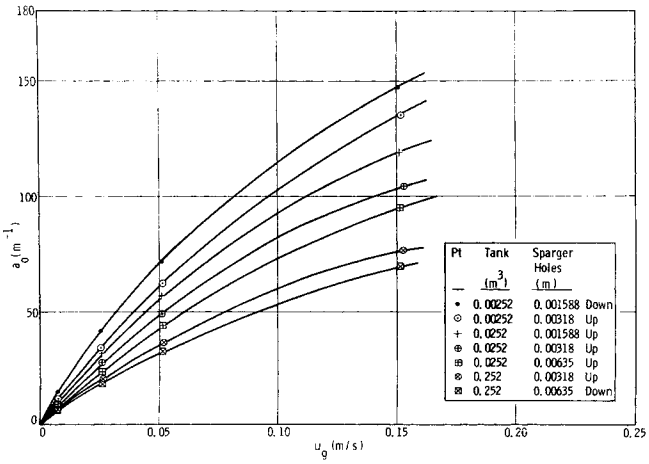

Fig. 12. a_o for gas sparging vs. superficial gas velocity u_g for air-water at 20°C.

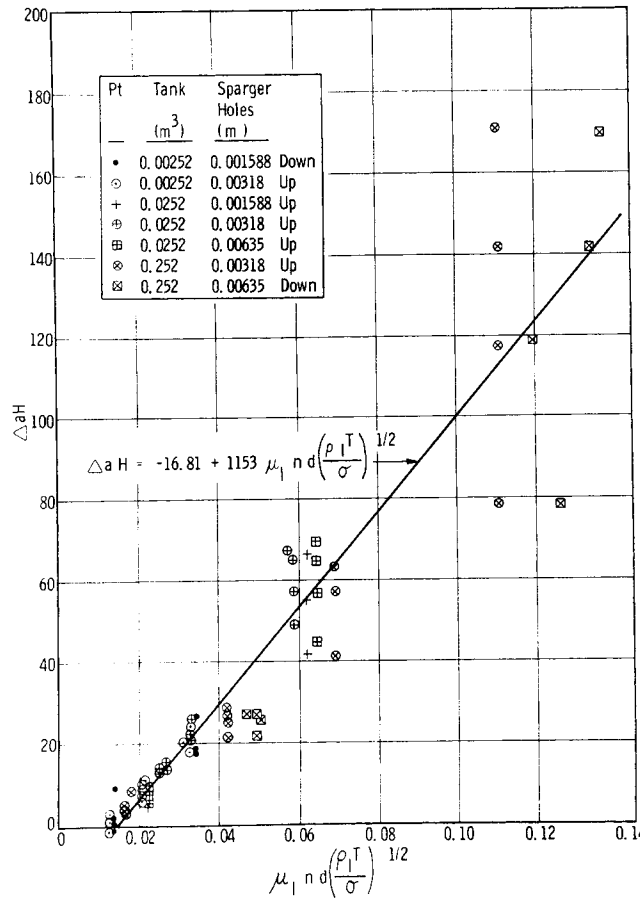

Fig. 13. ΔaH vs. $\mu_l\,nd\,(\rho_l T/\sigma)^{1/2}$.

through Equations (23) through (26).

Equations (16) through (19) provide the relationships needed to calculate the separate contributions and combined resultants of power inputs from gas sparging and mechanical agitation.

NOTATION

a = interfacial area per unit aerated volume, m^{-1}
a_o = interfacial area produced by gas sparging only, m^{-1}
Δa = incremental increase in interfacial area produced by mechanical agitation, m^{-1}
c = concentration, kg-mole/m³
c_i = inlet concentration, kg-mole/m³
c_o = outlet concentration, kg-mole/m³
c^* = interface concentration, kg-mole/m³
C_D = drag coefficient
C_1 = power input correction
C_2 = surface aeration correction
C_2u_g = superficial gas velocity including surface aeration, m/s
d = impeller diameter, m
d_o = sparger hole diameter, m
D = molecular diffusivity, m²/s
D_B = bubble diameter, m
D_{BE} = stable bubble diameter, m
D_{BM} = mean bubble diameter, m
D_{BO} = orifice bubble diameter, m
D_{VM} = Vermeulen bubble size, m
Ex = $\dfrac{g\,D_B\,(\rho_l - \rho_g)}{u_t^2\,\rho_l}$, expansion number
g = acceleration of gravity, m²/s

H = clear liquid depth, m
k = chemical rate constant, m³/kg-mole · s
k_L = mass transfer rate constant, m/s
$k_{L\,\text{calc}} = \left(\frac{4D}{\pi t_e}\right)^{1/2}$, calculated mass transfer rate constant, m/s
$k_{L\,\text{exp}} = k_L a/a$, experimental mass transfer rate constant, m/s
k_{LF} = Frössling mass transfer rate constant for rigid spheres, m/s
$k_L^* = k_{L\,\text{exp}}/k_{L\,\text{calc}}$, reduced mass transfer rate constant
M = gas molecular weight
n = agitator speed, s^{-1}, or reaction order
n_o = minimum agitator speed below which mechanical agitation has no influence on interfacial area, s^{-1}
N_o = number of sparger holes
N_o' = equivalent number of sparger holes
$N_{Pe} = \frac{D_{BM}\,u_t}{D}$, Peclet number
$N_{Reb} = \frac{D_{BM}\,u_t\rho_l}{\mu_l}$, bubble Reynolds number
$N_{Rei} = \frac{d^2 n\,\rho_l}{\mu_l}$, impeller Reynolds number
$N_{Reo} = \frac{Q_g\rho_l}{N_o d_o \mu_l}$, orifice Reynolds number
$N_{Sc} = \frac{\mu_l}{\rho_l D}$, Schmidt number
$N_{Sh} = \frac{k_L D_{BM}}{D}$, Sherwood number
$N_{SI} = \frac{\pi d n}{u_g}$, Strouhal number
$N_{Wei} = \frac{d^3 n^2 \rho_l}{\sigma}$, impeller Weber number
P_e = effective power input, W
P_g = power dissipated by sparged gas, W
P_m = aerated power input by mechanical agitation, W
P_{mo} = unaerated power input by mechanical agitation, W
P^*_{mo} = nonsparged power input by mechanical agitation corrected for top surface aeration, W
Q_g = gas flow rate, m³/s
Q_l = liquid flow rate, m³/s
R = gas constant, N · m/kg-mole · K
R_A^2 = square of the multiple correlation coefficient
t_e = exposure time for mass transfer, s
T = absolute temperature, K, or vessel diameter, m
u_g = actual superficial gas velocity, m/s
u_o = sparger hole velocity, m/s
u_t = bubble terminal velocity of rise, m/s
V = clear liquid volume, m³
V_a = aerated volume, m³
W = impeller width, m
X = sparger hole spacing, m
$Y = N_{SI}^{0.13}/Z^{0.87}$
Z = clear liquid depth above the impeller, m

Greek Letters

η = 0.06, fraction jet energy transmitted to bulk liquid
μ_g = gas viscosity, N · s/m²
μ_l = liquid viscosity, N · s/m²
π = absolute pressure, N/m²
π_o = pressure at sparger, N/m²
ρ_g = gas density, kg/m³
ρ_l = liquid density, kg/m³
σ = surface tension, N/m
ϕ = fraction gas holdup
ϕ_o = fraction gas holdup due to gas sparging only
ϕ' = Vermeulen correlation term for gas holdup
$\Delta\phi$ = incremental increase in fraction gas holdup produced by mechanical agitation
Φ = Vermeulen aeration correction

LITERATURE CITED

Astarita, G., *Mass Transfer with Chemical Reaction*, pp. 37-38, Elsevier, New York (1967).

Boussinesq, J., "Calculation of the Cooling Effects of Fluid Streams," *J. Math. Phys. Appl.*, **6**, 285 (1905).

Calderbank, P. H., "Physical Rate Processes in Industrial Fermentation, Part I: The Interfacial Area in Gas-Liquid Contacting with Mechanical Agitation," *Trans. Inst. Chem. Engrs.*, **37**, 443 (1958).

———., "Physical Rate Processes in Industrial Fermentation, Part II: Mass Transfer Coefficients in Gas-Liquid Contacting with and without Mechanical Agitation," *ibid.*, **38**, 173 (1959).

Clark, M. W., and T. Vermeulen, "Power Requirements for Mixing of Liquid-Gas Systems," pp. 29-31, Univ. California Lawrence Radiation Lab., Berkeley, UCRL-10996 (1963).

Datta, R. L., D. H. Napier, and D. M. Newitt, "The Properties and Behavior of Gas Bubbles Formed at a Circular Orifice," *Trans. Inst. Chem. Engrs.*, **28**, 14 (1960).

Frössling, N., "On the Vaporization of a Falling Drop," *Gerlands Beitr. Geophys.*, **52**, 170 (1938).

Haberman, W. L., and R. K. Morton, "An Investigation of the Drag and Shape of Air Bubbles Rising in Various Liquids," pp. 1-43, David Taylor Model Basin, Report 802, NR 715-702 (1953).

Hinze, J. O., "Fundamentals of the Hydrodynamic Mechanism Splitting in Dispersion Processes," *AIChE J.*, **1**, 289 (1955).

International Critical Tables, **4**, 447, McGraw-Hill, New York (1928a).

———, *ibid.*, **5**, 65 (1928b).

Lehrer, I. H., "Gas Agitation of Liquids," *Ind. Eng. Chem. Process Design Develop.*, **7**, 226 (1968).

———, "Gas Holdup and Interfacial Area in Sparged Vessels," *ibid.*, **10**, 37 (1971).

Leibson, I., E. G. Holcomb, A. G. Cacoso, and J. J. Jacmic, "Rate of Flow and Mechanics of Bubble Formation from Single Submerged Orifices," *AIChE J.*, **2**, 296 (1956).

Linek, V., "Determination of Interfacial Area in a Gas Sparged Reactor with Mechanical Agitation," *Chem. Eng. Sci.*, **21**, 777 (1966).

Mendelson, H. D., "The Prediction of Bubble Terminal Velocities from Wave Theory," *AIChE J.*, **13**, 250 (1967).

Michel, B. J., and S. A. Miller, "Power Requirements of Gas-Liquid Agitated Systems," *AIChE J.*, **8**, 262 (1962).

Miller, D. N., "Scale-Up of Agitated Vessels—Mass Transfer from Fixed Solute Surfaces," *Chem. Eng. Sci.*, **22**, 1617 (1967).

———., "Scale-Up of Agitated Vessels—Mass Transfer from Suspended Solute Particles", *Ind. Eng. Chem. Process Design Develop.*, **10**, 365 (1971).

O'Connel, F. P., and D. E. Mack, "Simple Turbines in Fully Baffled Tanks," *Chem. Eng. Progr.*, **46**, 358 (1950).

Peebles, F. H., and H. J. Garber, "Studies on the Motion of Gas Bubbles in Liquids," *ibid.*, **49**, 2 (1953).

Rushton, J. H., E. W. Costich, and H. J. Everett, "Power Characteristics of Mixing Impellers," *ibid.*, **46**, 467 (1950).

van Krevelen, D. W., and P. J. Hoftijzer, "Studies of Gas-Bubble Formation," *ibid.*, **46**, 29 (1950).

Vermeulen, T., G. M. Williams, and G. E. Langlois, "Interfacial Area in Liquid-Liquid and Gas-Liquid Agitation," *ibid.*, **51**, 85-F (1955).

Wesselingh, J. A., and A. C. van't Hoog, "Oxidation of Aqueous Sulfite Solutions: A Model Reaction for Measurements in Gas-Liquid Dispersions," *Trans. Inst. Chem. Engrs.*, **48**, T69 (1970).

Westerterp, K. R., L. L. van Dierendonck, and J. A. de Kraa, "Interfacial Areas in Gas-Liquid Contactors," *Chem. Eng. Sci.*, **18**, 157 (1963).

Manuscript received October 18, 1973; revision received and accepted January 23, 1974.